Optimum shell separation for closed axial cylindrical magnetic shields

Eugene Paperno[a)]
Department of Electrical and Computer Engineering, Ben-Gurion University of the Negev, P.O. Box 653, Beer-Sheva 84105, Israel

Saee Peliwal and Michael V. Romalis[b)]
Department of Physics, Princeton University, Princeton, New Jersey 08544

Anton Plotkin[c)]
Department of Electrical and Computer Engineering, Ben-Gurion University of the Negev, P.O. Box 653, Beer-Sheva 84105, Israel

(Presented on 8 November 2004; published online 17 May 2005)

The effect of shell separation on the axial shielding with closed double-shell cylindrical shields is investigated numerically. It is found that the optimum shell separation for practical, equal-thickness shields of the above type is considerably smaller than that for transverse spherical and infinitely long cylindrical shields: in most cases, air gaps equal 5%–10% of the inner shell diameter are wide enough to bring the shielding to 90% of its maximum. This indicates that closely spaced axial shields can be used without much sacrifice in performance. Taking into account the computed optimum shell separation for double-shell shields, one can easily optimize and design a compact and effective multishell shield. Based on the numerical study, an analytical approximation is suggested for the axial shielding with narrowly spaced double-shell cylindrical shields. © *2005 American Institute of Physics*. [DOI: 10.1063/1.1854254]

I. INTRODUCTION

Multishell cylindrical magnetic shields are an important part of experimental setups in modern fundamental physics where an extremely weak—down to 0.1 fT—level of magnetic disturbances and noise is required.[1] To obtain effective shielding with a compact enough multishell shield, the air gaps between the shield shells should be well optimized.

It is well known that for multishell magnetic shields, increasing the separation between the shells improves the shielding performance. For example, for two coaxial infinitely long cylindrical shells with the same thickness t, relative permeability μ_r, and diameters D_1 and D_2, such that $D_1 < D_2$, the transverse shielding factor is given by[2]

$$S_t \approx \frac{\mu_r^2 t^2}{D_1 D_2}\left(1 - \frac{D_1^2}{D_2^2}\right) \qquad (1)$$

for $\mu_r t / D_i \gg 1$. However, it is not usually practical to use widely separated shields because of the increased cost and space constrains in a given experiment. As shown in Fig. 1, for practical shields with equal thickness of the shells, the shielding performance rises quickly at first but then reaches a nearly constant value. Therefore, it is reasonable to define the optimum air gap, Δ_{opt}, as the smallest air gap that provides 90% of the maximum shielding. Separating shells with the Δ_{opt} air gaps rather than with that providing 100% shielding allows one to make the multishell shield much more compact, while not sacrificing too much of its shielding performance.

The optimum shell separation Δ_{opt} can be found analytically only for the simplest shielding assemblies, such as spherical and infinitely long cylindrical shields.[2] For example (see Fig. 1), an equal-mass double-shell spherical shield has $\Delta_{opt} = 15\%$ of D_1. A similar shield combined of long cylinders has $\Delta_{opt} = 24\%$. In a practical case, where the shell thickness is kept constant, a double-shell spherical and cylindrical shields have $\Delta_{opt} = 32\%$ and $\Delta_{opt} = 39\%$, correspondingly.

Existing literature suggests no treatment of Δ_{opt} for double-shell or multishell closed cylindrical shields. Shields of this type are most widely used in practice, and their shielding performance is typically limited by the axial shielding, since it is usually less effective than transverse

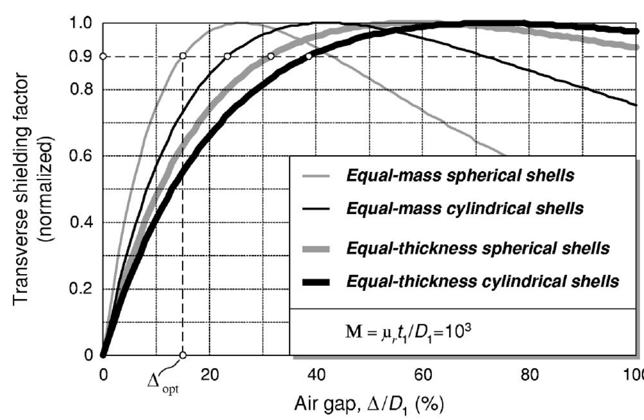

FIG. 1. The effect of the air gap $\Delta = (D_2 - D_1)/2$ on the shielding with double-shell spherical and infinitely long cylindrical magnetic shields. Equal-mass shields provide the most effective shielding per unit mass, but most practical shields are made using constant thickness material.

[a)]Electronic mail: paperno@ee.bgu.ac.il
[b)]Electronic mail: romalis@princeton.edu
[c)]Electronic mail: antonp@ee.bgu.ac.il

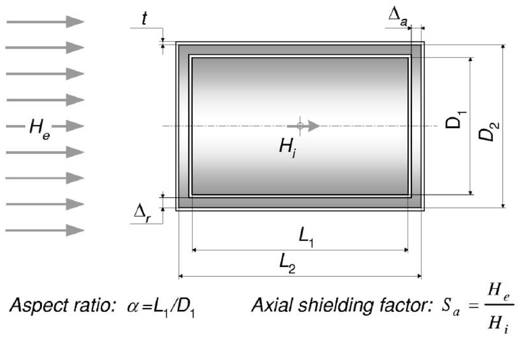

FIG. 2. Double-shell axial magnetic shield.

shielding. If a minimum level of shielding in all directions is desired, it is sufficient to optimize the shell separation focusing on the axial shielding factor.

In this work we make an effort to find numerically the optimum shell separation Δ_{opt} for closed double-shell axial cylindrical shields. Taking into account the computed Δ_{opt} for double-shell shields, one can easily optimize and design a compact and effective multishell shield.

We are also suggesting in this work an analytical approximation—that works well for very narrow air gaps—for the axial shielding with two closed cylindrical shells.

We have found that in contrast to spherical and infinitely long cylindrical shields, Δ_{opt} for equal-thickness closed axial cylindrical shields reaches surprisingly small values: it can be as small as 5% of D_1. Typical values of Δ_{opt} are about 8% and the maximum value of Δ_{opt} is about 17%. This indicates that narrowly spaced magnetic shields can be used without much sacrifice in performance.

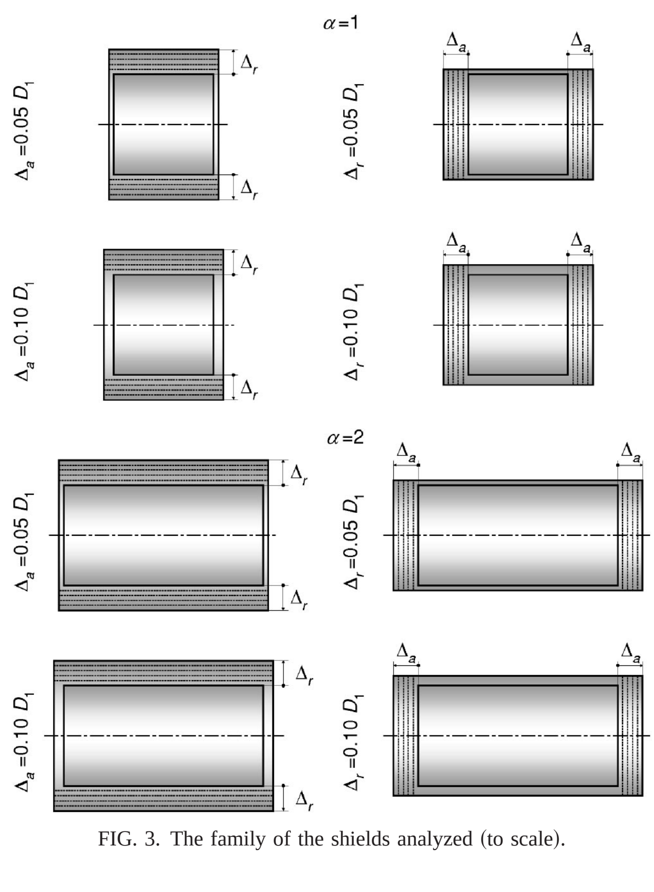

FIG. 3. The family of the shields analyzed (to scale).

II. NUMERICAL STUDY

A. Method

To investigate the effect of both the axial $\Delta_a=(L_2-L_1)/2$ and radial $\Delta_r=(D_2-D_1)/2$ air gaps on the axial shielding with closed double-shell cylindrical shields (see Fig. 2), we considered a family of the shields shown in Fig. 3. While composing this family, we assumed first that the inner shells having aspect ratios $\alpha=L_1/D_1$ of 1 and 2 will cover most possible applications: the inner shell having $\alpha=1$ will provide maximum shielding, because its shape is closest to the sphere, and the shells having $\alpha=2$ will provide a more compact design if an elongated area should be shielded. We assume that behavior of the shields having $1<\alpha<3$ will resemble that of the shields we analyze. We do not consider the shields with $\alpha<1$ or $\alpha>3$ since they are rarely used in practice.

The outer shells in Fig. 3 are separated from the inner shells either with fixed Δ_a and variable Δ_r (in the left column), or with fixed Δ_r and variable Δ_a (in the right column). The shell thickness was set at the same $t=1\%$ of D_1 value for the inner and outer shells. The normalized permeability of the shielding material $M=\mu_r t/D_1$ was set at 10^1, 10^2, and 10^3.

For each shield of Fig. 3, the axial shielding factor, defined in Fig. 2 as the ratio of the external uniform field and the field at the shield's center: $S_a=H_e/H_i$, was calculated numerically with the help of a finite element method (FEM) field simulator Maxwell® 2D made by Ansoft Corporation.

In our FEM modeling, we consider an axisymmetric linear magnetostatic case. Maxwell® 2D uses the Delaunay tessellation method to create a triangular mesh across the shield model, calculates the magnetic vector potential $\mathbf{A}_\phi$ at all points in the problem region, and determines from this the magnetic field $\mathbf{H}$ and magnetic field density $\mathbf{B}$. Maxwell® 2D is able to automatically refine the mesh in order to minimize the error energy in each element. In our simulations, we used such an adaptive meshing that provided a better than 1% convergence of the fields calculated.

B. Numerical results

The results of numerical calculations (see Fig. 4) reveal a strong dependence of the shielding factor S_a on both the axial Δ_a and radial Δ_r air gaps. This dependence is considerably stronger than that in Fig. 1 for transverse spherical and infinitely long cylindrical shields, especially if practical (equal-thickness) shields are considered. In most cases of Fig. 4, 5%–10% air gaps are wide enough to bring S_a to 90% of its maximum.

III. ANALYTICAL APPROXIMATION

In order to approximate the numerical results of Fig. 4, we suggest the following equation:

$$S_a \approx 0.52\frac{M^2/\alpha}{1+0.1/\Delta_a+0.06\alpha^2/\Delta_r}. \tag{2}$$

This equation was obtained intuitively as a result of efforts to match analytically the numerical results of Fig. 4. (Please

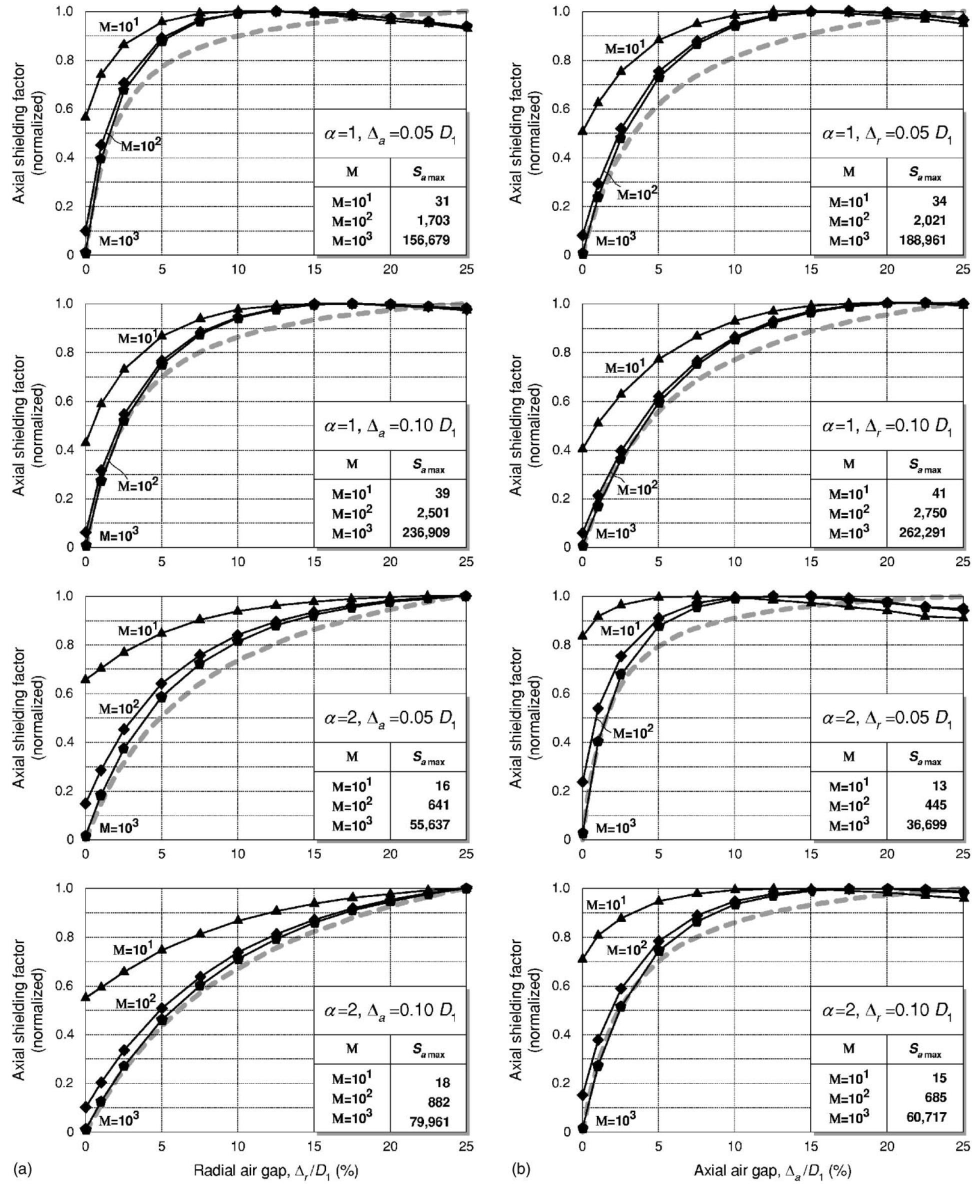

FIG. 4. The effect of the (a) radial and (b) axial air gap on the axial shielding factor for shields having different aspect ratios (α 1 and $\alpha=2$), different axial air gaps ($\Delta_a=5\%$ and 10% of D_1), and different normalized permeabilities ($M=10^1$, 10^2, and 10^3). The dashed lines represent the approximation with Eq. (2).

note that it is not our aim at the present stage to find the best possible analytical model for the effect we have discovered.)

One can use Eq. (2) to roughly estimate the axial shielding provided by two closed cylinders separated with either very narrow or relatively wide air gaps. Note that previously suggested equations, which are analyzed in Ref. 3, do not consider very narrow, smaller than 10% of D_1 air gaps.

IV. CONCLUSIONS

We have revealed in this work that optimum air gaps Δ_{opt} for practical (equal-thickness) double-shell closed axial cylindrical shields are considerably smaller than that for equal-thickness double-shell transverse spherical and infinitely long cylindrical shields. We show that in most cases, air gaps equal 5%–10% of the inner shell diameter are wide enough to bring the axial shielding with double-shell closed cylindrical shields to 90% of its maximum.

Taking into account the computed Δ_{opt} for double-shell shields, one can easily optimize and design a compact and effective multishell shield.

We emphasize that the effect of air gaps on the transverse shielding with finite-length cylindrical shields has not been analyzed in this work and will be the subject of future research.

ACKNOWLEDGMENTS

This work was supported in part by the Analog Devices, Inc., National Instruments, Inc., and Ivanier Center for Robotics Research and Production Management.

[1] I. K. Kominis, T. W. Kornack, J. C. Allred, and M. V. Romalis, Nature (London) **422**, 596 (2003).
[2] A. K. Thomas, IEEE Trans. Electromagn. Compat. **10**, 142 (1968).
[3] E. Paperno, H. Koide, and I. Sasada, J. Appl. Phys. **87**, 5959 (2000).